

X-ray Absorption Spectroscopy (XAS) Study of the Hydration Structure of Yttrium(III) Cations in Liquid and Glassy States: Eight or Nine-Fold Coordination?

Sofía Díaz-Moreno,[†] Adela Muñoz-Páez,^{*,‡} and Jesús Chaboy[§]

European Synchrotron Radiation Facility, 6, rue Jules Horowitz-BP 220, 38043 Grenoble CEDEX 9, France, Instituto de Ciencia de Materiales, Departamento de Química Inorgánica, CSIC–Universidad de Sevilla, c/Americo Vespucio s/n, 41092-Sevilla, Spain, and Instituto de Ciencia de Materiales de Aragón, CSIC–Universidad de Zaragoza, 50009 Zaragoza, Spain

Received: August 11, 1999; In Final Form: November 21, 1999

An extensive X-ray absorption spectroscopy study has been carried out on 0.005 to 2.0 molal $\text{YBr}_3 \cdot 6\text{H}_2\text{O}$ aqueous solutions in liquid and glassy states to determine the solvation structure of the yttrium(III) cations in aqueous dilute and concentrate solutions. The existence of a symmetric polyhedron of water molecules around yttrium(III) cations at 2.35 Å, as well as the absence of contact Y–Br ion pairs, in all of the investigated solutions was deduced from the EXAFS analysis. The existence of a multiple electron transition of nonnegligible intensity within the EXAFS region of the spectra has been proven. This transition induces an overestimation in the coordination numbers derived from the EXAFS analysis so that we have extended our study to the XANES part of the spectra. We have performed detailed computations of the XANES spectra by using a one-electron full-multiple-scattering code. This analysis shows unambiguously that the eight water molecules surround yttrium(III) cations at 2.35 Å forming a symmetric square antiprism.

Introduction

Several studies have been carried out in the last two decades trying to determine the hydration structure of different cations in solution, making use of techniques such as neutron diffraction, X-ray diffraction, and extended X-ray absorption fine structure (EXAFS) spectroscopy.^{1–3} The structures of some of them are still unresolved, such as that of yttrium(III) cation, which is relatively small and highly charged. Traditionally, the structural chemistry of this cation has been compared with that of the heavy lanthanides, essentially due to the fact that its ionic radius (1.02 Å) is very close to the values found for third-valent cations at the end of the rare earth series (e.g., Tm^{3+} 0.99 Å, Er^{3+} 1.00 Å, Tb^{3+} 1.04 Å) when observed in systems with 8-fold coordination.^{4,5} To place the liquid-state complexation of yttrium(III) in context, it is advantageous to consider its coordination in a range of solid-state compounds. Most of the yttrium solid compounds are isomorphous with those of the lanthanide series and display a large number of different coordination environments. For example, in $[\text{Y}(\text{H}_2\text{O})_8][\text{CF}_3\text{SO}_3]_3$, the yttrium(III) cations are surrounded by nine water molecules forming a tricapped trigonal prism,⁶ while in $[\text{Y}(\text{H}_2\text{O})_8][\text{Tc}_2\text{Cl}_8] \cdot \text{H}_2\text{O}$ the yttrium(III) cation has a local environment where eight hydration water molecules form a square antiprism around the cation.⁷ In the case of the compound $[\text{Y}(\text{H}_2\text{O})_8]\text{Cl}_3 \cdot 2\text{C}_{10}\text{H}_8\text{N}_2$ the cation is again 8-fold coordinated, but in contrast with the previous case, the water molecules are located so as to form a distorted dodecahedron.⁸ Another possible coordination geometry adopted by this cation is a distorted octahedron,⁹ as in the case of YCl_3 , or a symmetric one, as in the case of $[\text{But}_4\text{N}][\text{Y}(\text{NCS})_6]$.¹⁰ It can be deduced

through a comparison of these structures that the coordination number and the polyhedron adopted by this cation depend strongly not only on the coordinating atom but also on the packing forces in the crystal and on the hydrogen bond network that can be formed.

Though the coordination of yttrium(III) in the solid state has been extensively studied, the in-solution coordination structure is not well established. Thus, a study using X-ray diffraction found that the yttrium(III) cations were surrounded by 8.0 ± 0.3 water molecules at 2.33 and 2.36 Å in concentrated aqueous solutions of yttrium selenate and perchlorate, respectively.¹¹ In another study, by using anomalous X-ray scattering (AXS) to study 1.0 M and 0.5 M YCl_3 aqueous solutions, 8.2 ± 0.5 water molecules were localized at approximately 2.46 Å from the central yttrium(III) cation showing also evidence for the formation of some contact ion pairs relating Y^{3+} and Cl^- ions.¹² An additional study of yttrium(III) hydration by means of EXAFS of concentrated aqueous solutions of YBr_3 and YCl_3 obtained Y–O_{water} distances equal to 2.33 Å in eight coordinated hydrates, but no evidence of coordinating halide ions was found.¹³ The aforementioned studies only provide information regarding concentrated solutions. However, to determine the role of solute–solute interactions, if any, in the formation of hydration complexes, it is important to investigate the hydration structure in dilute and highly dilute solutions. In addition, no specific hydration polyhedron has yet been proposed and there is no complete agreement about the interatomic distance for Y–O_{water}, with quoted values varying from 2.33 and 2.46 Å.

In the present work, taking advantage of the capability of the techniques to be used in a wide range of concentrations, we use EXAFS and X-ray absorption near edge structure (XANES) spectroscopies to determine the solvation structure of the yttrium(III) cation in aqueous dilute and concentrate solutions. Both techniques are complementary since the first

* Corresponding author: e-mail, adela@cica.es; fax number, 34-95-4460665.

[†] European Synchrotron Radiation Facility.

[‡] CSIC–Universidad de Sevilla.

[§] CSIC–Universidad de Zaragoza.

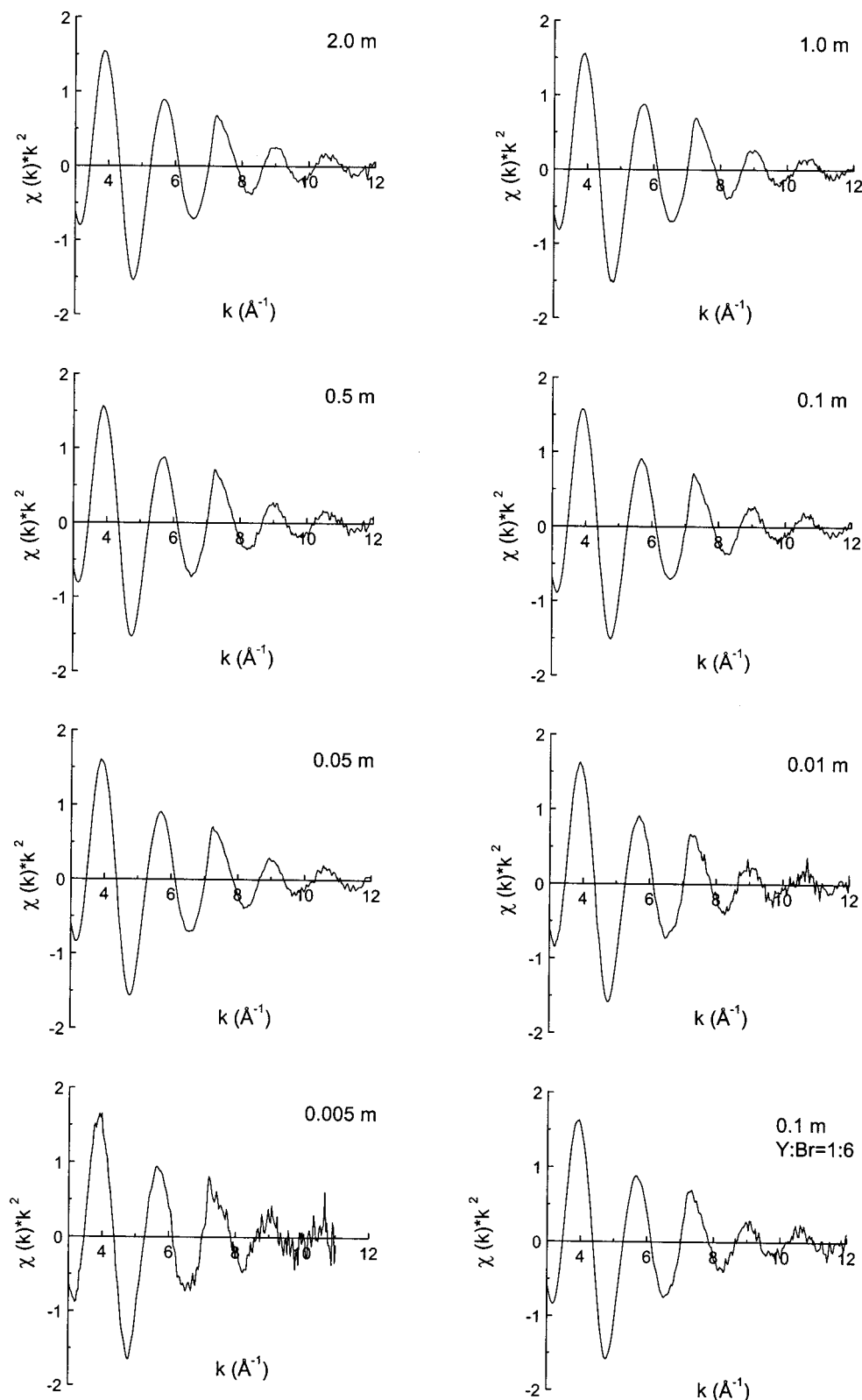


Figure 1. k^2 -weighted Y K-edge raw EXAFS spectra of YBr_3 liquid aqueous solutions of the indicated concentrations.

provides accurate information about next neighbors coordination distances and coordination numbers, while the second is especially sensitive to the coordination polyhedra. The main aims are to investigate both the polyhedra formed by water molecules around this cation, and the possible formation of ion pair structures. To this end, XAS measurements have been performed at the Y K-edge varying the cation concentration and the cation:anion ratio, this last obtained by adding a salt

containing the same anion. Additionally, to decrease the thermal fluctuation and to examine the possible distortion in the hydration polyhedra, a thermally quenched liquid system was measured. For comparative purposes, a solid compound of known structure, $[\text{Y}(\text{H}_2\text{O})_9][\text{CF}_3\text{SO}_3]_3$, was investigated as well. The experimental spectra have been compared with ab initio EXAFS and XANES spectra computed for the different proposed arrangements.¹⁴

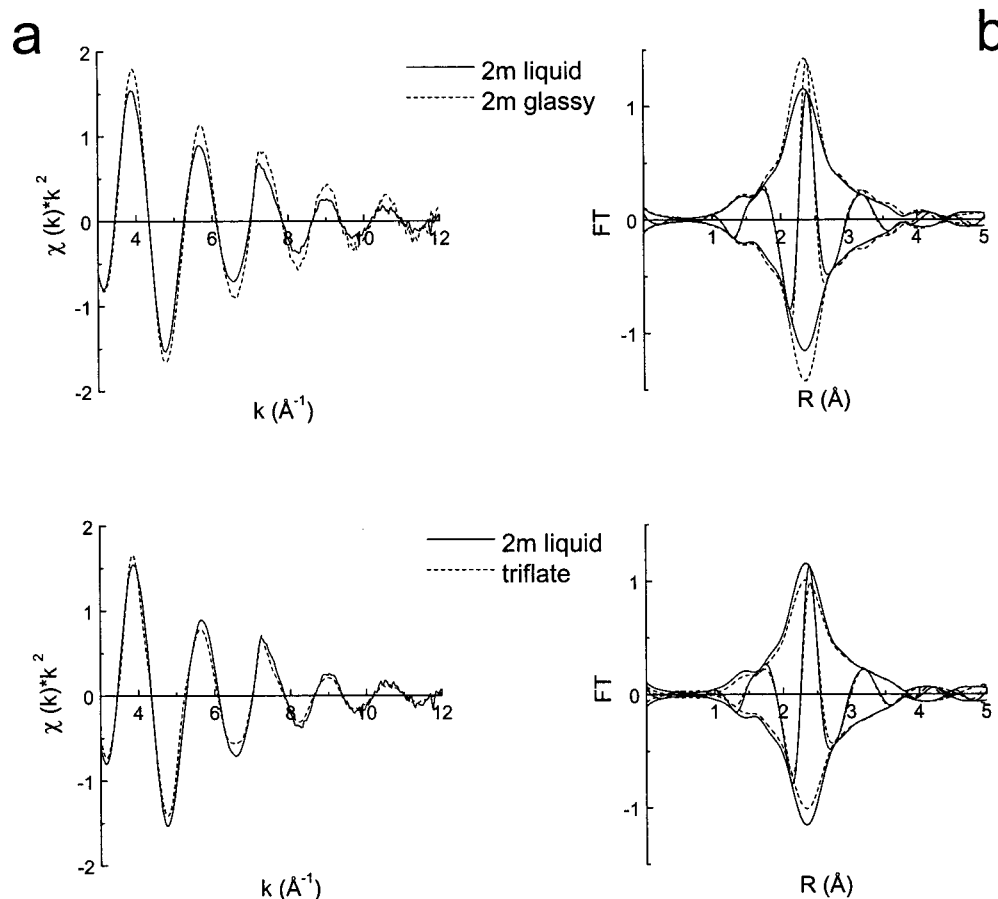


Figure 2. (a) Comparative plots of the EXAFS spectrum of YBr_3 2 m aqueous solution in liquid state (solid line), with the corresponding spectrum of the glassy sample recorded at liquid nitrogen temperature (dashed line) and with the spectrum of yttrium(III) triflate (dotted line). (b) Magnitude and imaginary part of the Fourier transform (k^2 , $\Delta k = 3.2\text{--}12 \text{ \AA}^{-1}$) Y–O phase shift corrected of the spectra included in Figure 2a.

Experimental Section

(a) Sample Preparation. Yttrium(III) bromide hexahydrate, $\text{YBr}_3 \cdot 6\text{H}_2\text{O}$, in the solid state was prepared from commercial Y_2O_3 (99.99% Aldrich Chemical Co., Inc.) through dissolution in a minimum volume of 48% HBr. The solution was then evaporated in a sand bath until crystallization occurred. The so produced white crystals were then separated using a sintered glass filter and were kept in a desiccator over Al_2O_3 .¹⁵

From this compound, aqueous solutions of concentrations 2.0, 1.0, 0.5, 0.1, 0.05, 0.01, and 0.005 m were prepared. To avoid hydrolysis of the samples, which could lead to the appearance of other species in solution such as $[\text{Y}(\text{OH})(\text{H}_2\text{O})_n]^{2+}$, the pH of all the solutions was kept constant at $\text{pH} = 1.0$ by adding the required amount of HClO_4 . To study the formation of ion pair structures, aqueous solutions with a ratio Y:Br equal to 1:6 and 1:9 were prepared by adding NaBr salt to the 0.1 M YBr_3 aqueous solution.

A glassy sample of a YBr_3 2.0 m solution was prepared by quick immersion of the corresponding aqueous solution into liquid nitrogen and it was kept at this temperature in a vacuum cryostat. The vitrification was visually confirmed by checking the optical transparency. Solutions of lower concentration did not yield vitrified samples, probably due to separate crystallization of the solute and/or the solvent. To keep unaltered the hydration structure around yttrium(III) cations no additive, such as glycerol,¹⁶ was used to prevent crystallization. The cooling rate in the present study was estimated to be approximately 400 K/min.¹⁷

The solid compound enneahydratedyttrium(III) trifluorometanesulfonate, hereafter abbreviated as yttrium(III) triflate,

$[\text{Y}(\text{H}_2\text{O})_9][\text{CF}_3\text{SO}_3]_3$, was also prepared following the method proposed by Harrowfield et al.⁶ This solid was used as a model compound against which comparisons could be made since its hydration structure is well known.

(b) Measurements of X-ray Absorption Spectra and Data Analysis. X-ray absorption spectra at the yttrium K-edge (17038 eV) were measured at the EXAFS station BL10B of the Photon Factory (National Laboratory for High Energy Physics (KEK), Japan). The storage ring was operated at 2.5 GeV, with a current of 300 mA. The calibration of the spectrometer was carried out using a 25 μm thick niobium foil. All measurements, except that of the glassy sample measured at 77 K in a vacuum cryostat, were performed at room temperature in transmission mode, using ion chambers as detectors and a Si(311) channel-cut monochromator. The ion chambers were filled with a He/Ar gas mixture and optimized to absorb 20% of the beam intensity in I_0 and 80% in I_t . Each data point was collected for 1 s and several scans were averaged, to improve statistical quality.

The liquid samples were measured in a specially designed cell, allowing for variable path lengths.¹⁸ This is necessary for optimization of the absorption edge jump. The solid compound yttrium(III) triflate was measured in a sample holder covered by Kapton, and placed in a hermetically sealed plastic bag, as this sample is very hygroscopic.

(c) EXAFS Data Analysis and XANES Computations. Standard procedures were used to perform background removal prior to analysis of the EXAFS regions of the spectra.¹⁹ The onset energy of the absorption process was chosen to be the maximum of the first derivative in the edge region of the absorption spectrum.

TABLE 1: EXAFS First Hydration Shell Parameters (Y—O_{water}) Found for YBr₃·6H₂O Aqueous Solution of the Indicated Concentrations (k^2)^a

sample	N	$\Delta\sigma^2$	$R/\text{\AA}$	$\Delta E_0/\text{eV}$
2.0 m	8.6 ± 0.1	0.0075 ± 0.0003	2.353 ± 0.001	3.0 ± 0.1
1.0 m	8.5 ± 0.1	0.0075 ± 0.0003	2.353 ± 0.001	2.8 ± 0.1
0.5 m	8.6 ± 0.1	0.0077 ± 0.0003	2.353 ± 0.001	2.8 ± 0.1
0.1 m	8.6 ± 0.1	0.0076 ± 0.0003	2.353 ± 0.001	2.6 ± 0.1
0.05 m	8.6 ± 0.1	0.0074 ± 0.0003	2.352 ± 0.001	2.7 ± 0.1
0.01 m	8.7 ± 0.14	0.0075 ± 0.0003	2.352 ± 0.002	2.9 ± 0.1
0.005 m	8.8 ± 0.2	0.0076 ± 0.0003	2.352 ± 0.003	2.8 ± 0.2
0.1 m; Y:Br = 1:6	8.6 ± 0.14	0.0076 ± 0.0004	2.351 ± 0.002	2.6 ± 0.2
0.1 m; Y:Br = 1:9	8.5 ± 0.23	0.0070 ± 0.0007	2.349 ± 0.003	2.9 ± 0.2
2.0 m; glassy	8.75 ± 0.04	0.0052 ± 0.0001	2.351 ± 0.001	2.8 ± 0.1
triflate(s)	5.80	0.0059	2.342	1.6
	2.90	0.0069	2.461	3.3

^a *N*, coordination number; $\Delta\sigma^2$, Debye–Waller factor; *R*, coordination distance; ΔE_0 , inner potential correction. Standard deviations were calculated from the covariance matrix and estimates of the noise level in the scans.

The EXAFS spectra were analyzed with the program XDAP (University of Utrecht),²⁰ which uses a nonlinear least-squares fitting algorithm. Errors in the structural parameters were calculated from the covariance matrix taking into account the statistical noise in the experimental EXAFS spectra as well as the correlations between the refined parameters. Fit quality was determined using the goodness of fit value (ϵ_ν^2) outlined in the workshop for “Standards and criteria for EXAFS data analysis”.²¹ Phase shifts and backscattering amplitude functions for Y—O pairs were determined from the algorithm of Rehr et al.²² (FEFF 7.02 code). The amplitude reduction factor, S_0^2 , and the Debye–Waller factor, σ^2 , governing the thermal and structural disorder, were taken as 1.0 and 0.0, respectively.

The computation of the XANES spectra was carried out using the multiple-scattering CONTINUUM code²³ based on a one-electron full-multiple-scattering theory.²⁴ A detailed description of the method used can be found elsewhere.²⁵ The calculation of the Y K-edge absorption cross-section requires an inner core orbital calculated in a ground state potential and the solution of the scattering problem in the excited state (1 s core hole) potential. The cluster potential was approximated by a set of spherically averaged muffin-tin potentials, which were built by following the standard Mattheis’ prescription.²⁶ The Coulombic part of each atomic potential was generated using densities for neutral atoms obtained from the tabulated atomic wave functions by Clementi and Roetti.²⁷ For the ground-state potential, the atomic orbitals were chosen to be neutral while different choices were used to build the final state potential. Self-consistent field potential, in which the final state potential is calculated by promoting a 1s electron of the photoabsorber to its outer shell and fixing the 1s occupancy during the self-consistent field procedure, yielded the best results. The construction of the scattering potential needs the addition of an exchange and correlation potential. In this work, we have used the classical Slater X_α approach,²⁸ the energy dependent potentials of Hedin–Lundqvist,²⁹ and the Dirac–Hara exchange,³⁰ this last showing the best agreement with the experimental data.

Results and Discussion

EXAFS Analysis. The raw EXAFS data of the YBr₃·6H₂O aqueous solutions of concentrations 0.005 M up to 2.0 m are shown in Figure 1. It can be seen that all of the spectra are very similar, both in amplitude and phase. This figure also includes the raw EXAFS function corresponding to the 0.1 M aqueous solution of YBr₃·6H₂O with a ratio Y:Br = 1:6. The features observed in this spectrum are quite similar to those of the spectra corresponding to the solutions of the same concentration with different Y:Br ratios.

TABLE 2: Data Analysis Parameters^a

sample	$\Delta k/\text{\AA}$	noise amplitude	ϵ_ν^2	ν
2.0 m	3.2–12.0	0.002	5.45	19.3
1.0 m	3.2–12.0	0.002	6.25	19.3
0.5 m	3.2–12.0	0.002	5.52	19.3
0.1 m	3.2–12.0	0.002	5.59	19.3
0.05 m	3.2–12.0	0.002	8.43	19.3
0.01 m	3.2–9.5	0.003	4.74	13.7
0.005 m	3.2–9.5	0.004	2.53	13.2
0.1 m; Y:Br = 1:6	3.2–12.0	0.003	3.68	19.3
0.1 m; Y:Br = 1:9	3.2–8.7	0.005	2.22	11.3
2.0 m, glassy	3.2–12.0	0.001	41.0	19.3
triflate(s)	3.2–14.0	0.001	36.0	24.1

^a Noise amplitude for $\chi(k)$; ϵ_ν^2 , goodness of fit; ν , degrees of freedom.

Figure 2 shows comparative plots in *k*- (Figure 2a) and *r*-space (Figure 2b), of the 2.0 m aqueous solutions recorded at room temperature in liquid state, with the spectra of the same solution recorded at liquid nitrogen temperature in the glassy state (upper part) and with the spectra of the yttrium(III) triflate recorded in solid state at room temperature (lower part). As expected, the amplitude of the EXAFS spectrum of the sample recorded at liquid nitrogen temperature is higher than that of the sample recorded at room temperature. Although no significant differences appear between the EXAFS signals of the triflate and the liquid solution, the amplitude of the Fourier transform of the triflate is smaller. In all cases a single peak appears in the FT at around 2.3 Å, thus indicating that there is only a significant contribution. No additional contribution appears in the glassy sample indicating that the quenching of the sample does not induce medium range order.

As seen in Table 1, the values obtained for the coordination numbers, *N*, Debye–Waller factors, $\sigma^2(\text{\AA}^2)$, interatomic distance Y—O_{water}, *R*(Å), and inner potential correction, $\Delta E_0(\text{eV})$, for the different solutions of YBr₃·6H₂O are the same within error, 8.6, 0.0075 Å², 2.35 Å and 2.7 eV, respectively, for all the liquid samples. For the glassy solution, the value of the Debye–Waller factor is notably smaller ($\approx 40\%$) than in the previous cases. This decrease is due to the lower temperature, since the motions of ions and water molecules are drastically decreased in the quenched solutions, the main contribution to the Debye–Waller factor being that corresponding to the static disorder of the hydration shell. Other authors have already observed a similar decrease in the Debye–Waller factors of quenched solutions of similar systems.¹⁷ The values of the rest of parameters, *N*, *R*, and ΔE_0 , are very similar to those found for the liquid solutions, thus indicating that the polyhedron formed by the water molecules around yttrium(III) cations in this quenched

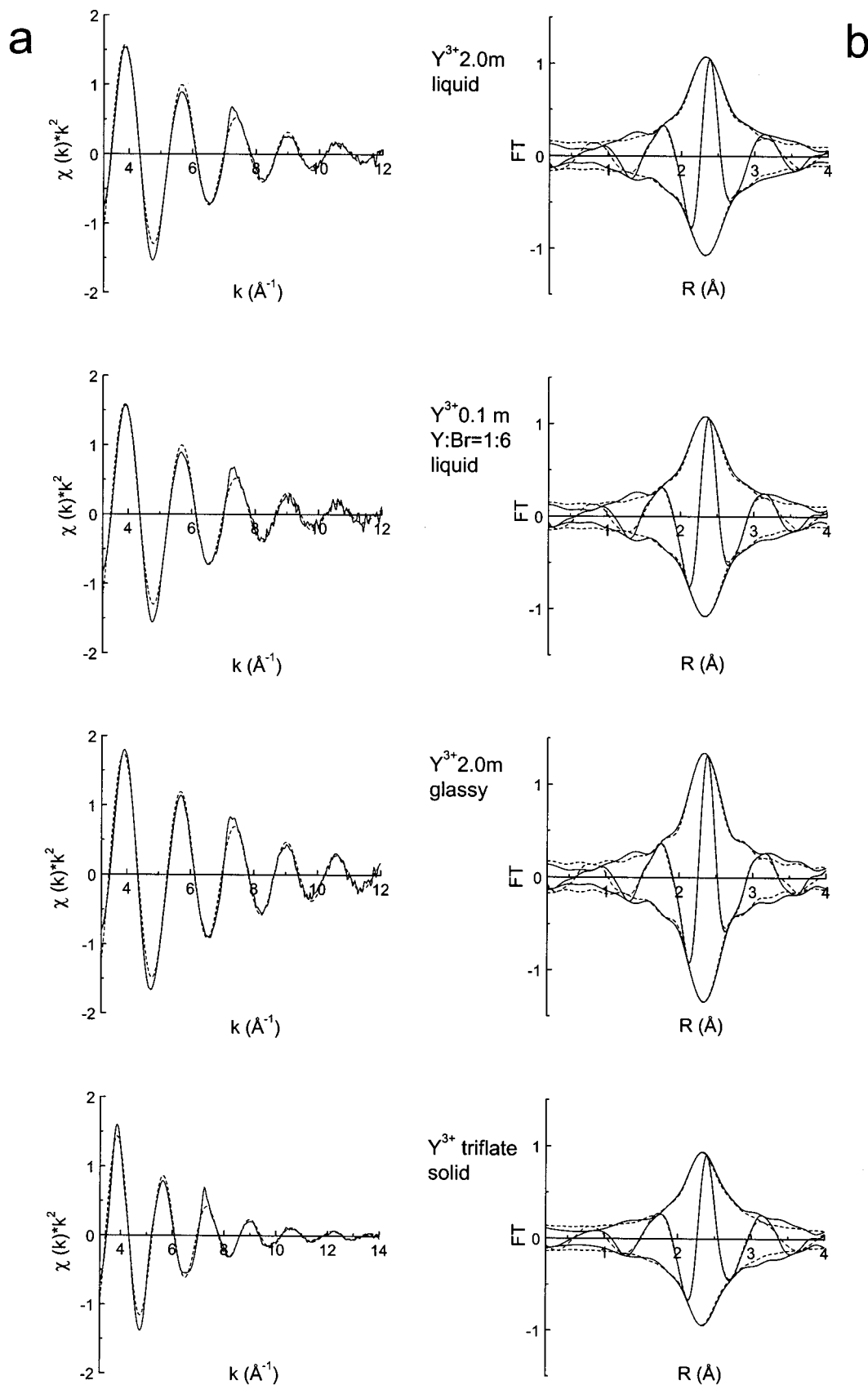


Figure 3. (a) k^2 -weighted raw EXAFS data (solid line) and best fit with parameters of Table 1 (dashed line) of the liquid solutions 2 m in YBr_3 ; 0.1 m in YBr_3 , and 0.1 m in NaBr_3 , of the solution 2 m in YBr_3 in the glassy state, recorded at liquid nitrogen temperature, of the solid compound yttrium(III) triflate. (b) Magnitude and imaginary part of the Y–O phase shift corrected k^2 -Fourier transform of the spectra included in Figure 3a (see Table 2 for Fourier transform ranges).

solution is the same to that found in the liquid state. Additional information about the analysis is included in Table 2.

The spectrum of the triflate deserves further comment. Although it is rather similar to that of the glassy and to

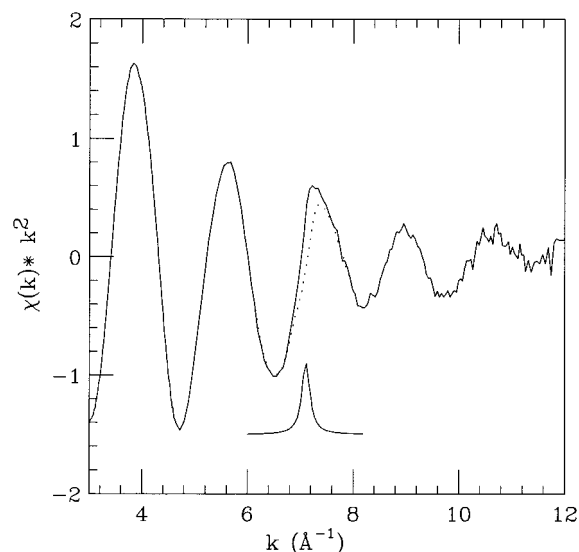


Figure 4. k^2 -weighted raw EXAFS data of YBr_3 2.0 M liquid aqueous solution prior (solid line) and after subtracting the multielectron contribution (dots) which is shown at the bottom.

that of the liquid aqueous solution (see Figure 2), the small differences existing between these spectra require different approaches during the analysis. Indeed, a fit similar to that carried out in these samples, using a unique oxygen atom shell (results not included in the table) yielded a coordination number smaller than 9 (≈ 7), while the Debye–Waller factor found was larger than those of the aqueous solutions. In contrast, a good reproduction of the spectrum was obtained using the structural parameters of the crystalline hydrate forming a tricapped trigonal prism,⁶ with six prismatic water molecules and three capping molecules at a longer distances (see parameters in Table 1). With this arrangement the elongation in the distances of the capping water molecules generates destructive interference, and the amplitude of the resulting EXAFS function is smaller than the sum of the contributions of the two shells. Since a similar phenomenon of destructive interference does not appear in the glassy or liquid sample, it might be concluded that the hydration polyhedra in these systems are symmetric, and we postulate that they should be the same, the only difference being the smaller thermal motion in the glassy sample.

Lacking direct structural information about solvation structure in solution, the structure of the crystalline hydrates, as determined by XRD, has been taken as the best model for solvation structures.^{31,32} This assumption seems to work well in cations showing well-defined octahedral or tetrahedral solvates,³¹ but has been questioned for the case of the heavy elements of the lanthanide series,^{33,34} to which yttrium(III) has compared. Similarly, scandium(III) cations are nine-coordinated in solid triflate, while recently it has been shown by EXAFS and XRD that they are surrounded by about seven water molecules in liquid aqueous solutions.³⁵ The previous EXAFS results point to a similar situation for yttrium(III) hydrates, showing different polyhedra in solution and in the solid-state crystalline hydrate.

Figure 3 shows the raw EXAFS data and the Fourier transforms for the 2.0 m aqueous solution of $\text{YBr}_3 \cdot 6\text{H}_2\text{O}$, the 0.1 m aqueous solution with Y:Br ratio 1:6, the model compound yttrium(III) triflate, and the glassy solution together with their best fits obtained using the parameters included in Table 1. Note the good agreement between experimental and calculated spectra, both in k - and r -space in all cases, with the only exception being the disagreement appearing at around 7.5

Å, where there seems to be a contribution not accounted for by calculations, which adds to the EXAFS oscillation.

The contribution appears in all of the investigated systems and its intensity does not seem to be affected by the chemical environment or by the aggregation state, since it appears even in the glassy sample and in the solid triflate. This is a first indication of the atomic-like character of this feature. Moreover, since it cannot be accounted for within a single electron framework, it seems natural to attribute this structure to a multielectron process. In such a class of processes a second electron is ejected from the core together with the 1s electron, giving rise to unphysical structures on the EXAFS spectra. We have performed explicit calculations of the allowed transitions and found that it is due to double $1s3d \rightarrow 5p4d$ transition.^{36,37} The calculated energy for the transition is 185.12 eV above the main $1s \rightarrow 5p$ transition and its intensity relative to that of the white line of the main transition is estimated to be 2%, both values in excellent agreement with experimental data. For the sake of completeness we report in Figure 4 the calculated multielectron process contribution showing as an example how its subtraction modifies the EXAFS signal in the case of the 2.0 m aqueous solution.

From the best fits results of the EXAFS spectra it can be concluded that the hydration structure around the yttrium(III) cation does not change with the concentration of the solution in the range between 2.0 and 0.005 m, or with the Y:Br ratio within the range 1:3 to 1:9. Moreover, the agreement of the EXAFS parameters for all the solutions is excellent.

Since the structural parameters are the same for all of the solutions, even when the Y:Br ratio is 1:9, we can discard the existence of inner-sphere complexes, where the Br^- anions would come into the first coordination sphere of the cation. We note that the fit obtained when considering one coordination sphere of oxygen atoms is rather good and the differences in the phase shifts and the backscattering amplitude functions of Y–O and Y–Br are large enough for the EXAFS technique to distinguish both contributions. This has been demonstrated in the case of the chloroaquocomplexes of chromium, where the capabilities of the EXAFS technique to distinguish Cr–O and Cr–Cl contributions in the first and second coordination sphere have been shown.³⁸ The existence of inner-sphere complexes involving Br^- anion was first postulated for concentrated solutions of ErBr_3 using X-ray diffraction.³⁹ Recently, direct evidence of this sort of complex was obtained by EXAFS in solutions of thulium(III)⁴⁰ and yttrium(III)⁴¹ bromide in dimethylformamide (DMF)–dimethylacetamide (DMA) mixtures, and by using NMR in YBr_3 solutions in the same type of solvents.⁴² Moreover we have not found evidence of the presence of solvent-separated $\text{Y}^{3+} \text{--} \text{Br}^-$ ion pairs in either in the liquid state or in the glassy system. This might be due either to the fact that they do not exist, or to the fact that the technique is not sensitive enough to detect this type of weakly bonded species.

Concerning the main aim of this work, the determination of the hydration polyhedra around yttrium(III) cations, the EXAFS analysis here presented yields accurate information regarding coordination distances, 2.352 ± 0.001 Å. In contrast, the results are not conclusive regarding the coordination number, as an average value of 8.6 has been obtained. These results agree quite reasonably with previous studies of yttrium(III) hydration structure,^{11–13} and with the results obtained for the heavier lanthanides.¹⁷ Nevertheless, they do not confirm the result of another study according to which all of the lanthanide cations are surrounded by twelve water molecules in aqueous solu-

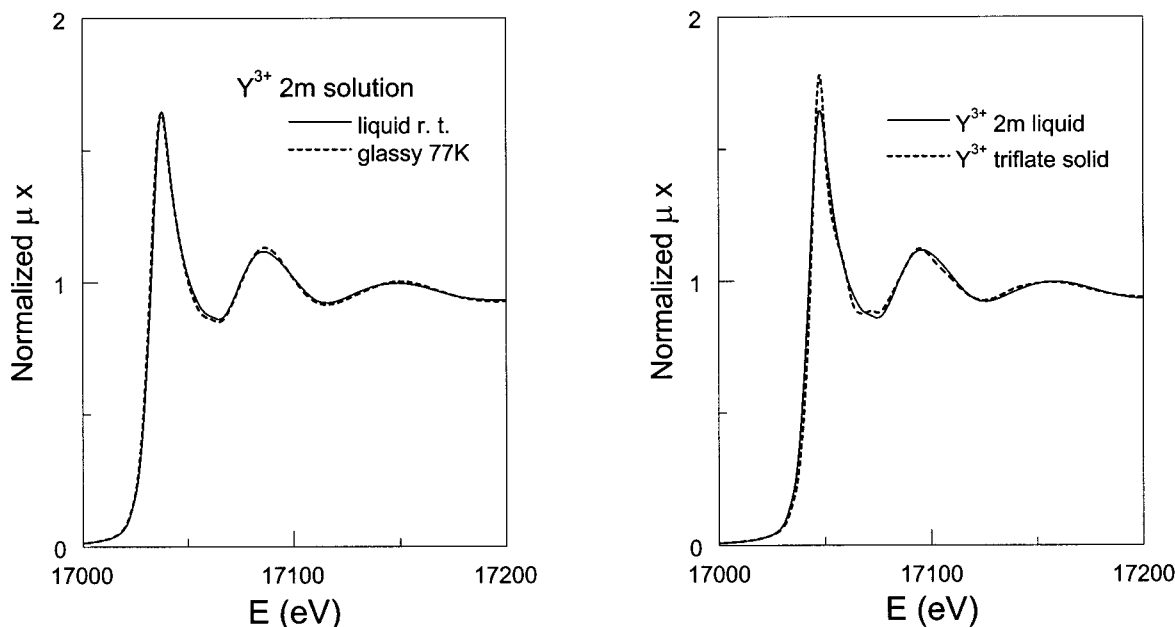


Figure 5. Y K-edge normalized XANES spectra of 2 m YBr_3 aqueous solution in liquid state (solid line), of the same solution in the glassy state (dashed line), and of the solid compound yttrium(III) triflate (dashed line).

tions.⁴³ Except this last work, from literature results discussed above and from the data presented here, both the nine- and eight-coordinated environments are suitable to describe the hydration structure of yttrium(III) cations. The most stable 9-fold coordinated polyhedron is the tricapped trigonal prism, which needs a larger splitting between capping and prismatic water molecules when the radius of the central cation is smaller,³³ while the most stable polyhedron for the 8-fold coordination is the symmetric square antiprism.

It should be noted, however, that the indetermination in the coordination numbers is partially due to the presence of a multielectron process superimposed to the EXAFS oscillations. Previous works have shown that the error introduced into the coordination numbers by neglecting the presence of double-electron transitions might be as high as 10%.^{36,37} The presence of such double-electron excitations have been shown in numerous rare earth L_{III} -edge^{36,37,44} spectra. Systems containing other cations show similar transitions in K-edges as well. For instance, such a double transition appears in the Y K-edge, although it is partially buried in the rather complex spectrum of $[\text{Y}(\text{NCS})_6]^{3-}$;¹⁰ in contrast it is clearly visible in the EXAFS raw data of YCl_3 and YBr_3 aqueous solution¹³ and in Rb-K edge spectra of bile acid Rubidium salts.⁴⁵ In our case, the double electron transitions appear in such a position as to increase the total intensity of the signal, so that the coordination numbers derived from the standard EXAFS analysis above are overestimated. This fact together with the requirement of a symmetric environment, as deduced from the comparison of the solution and triflate spectra, suggests that the most probably hydration structure of yttrium(III) cations is formed by eight water molecules localized in a square antiprism. However, to get a deeper insight on this subject, we have carried out the *ab initio* simulation of the XANES part of the XAS spectra.

XANES Analysis. Since the XANES region is very sensitive to the coordination polyhedra, its analysis might confirm the proposed eight coordination for the hydration polyhedra around yttrium(III) cations in aqueous solution. Figure 5a shows comparative plots of the XANES spectrum of the 2 m solution in liquid and glassy state, while Figure 5b shows comparative plots of the liquid solution and the solid triflate. The spectra of

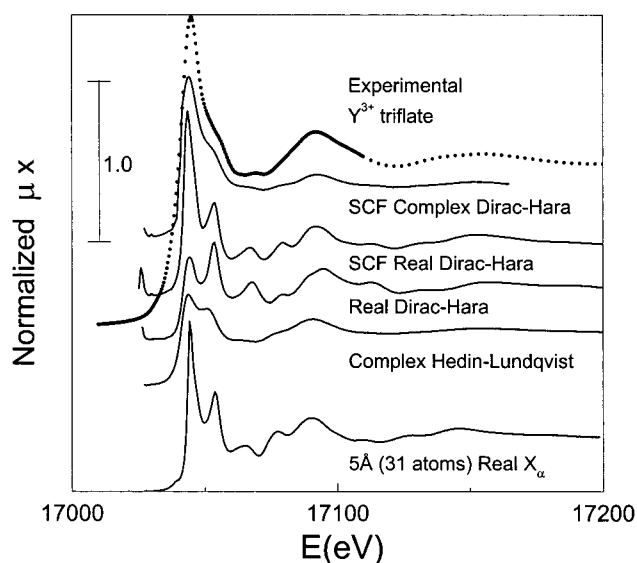


Figure 6. Experimental XANES spectra of yttrium(III) triflate (dotted line) versus the spectra computed (solid line) for a 31-atom cluster using the indicated potentials (for computation details see text).

the liquid and glassy solution superimpose, thus confirming that the coordination polyhedra are the same and indicating that the XANES region is less sensitive to the disorder than the EXAFS one (look at the higher amplitude of the EXAFS oscillations in the glassy sample in Figure 2a). In contrast, some differences appear between the spectra of the triflate and that of the liquid solution, i.e., higher intensity of the white line and the appearance of a small shoulder in the high energy side of the white line. This points to the existence of a different coordination polyhedra in this solid system, as already deduced from the analysis of the EXAFS data. To obtain precise information, several computations were carried out to reproduce this region of the spectrum.

The performance of the calculations has been tested on the solid yttrium(III) triflate. Figure 6 shows the comparison of the experimental spectrum of this compound and the result of the calculations carried out considering a cluster of 31 atoms around

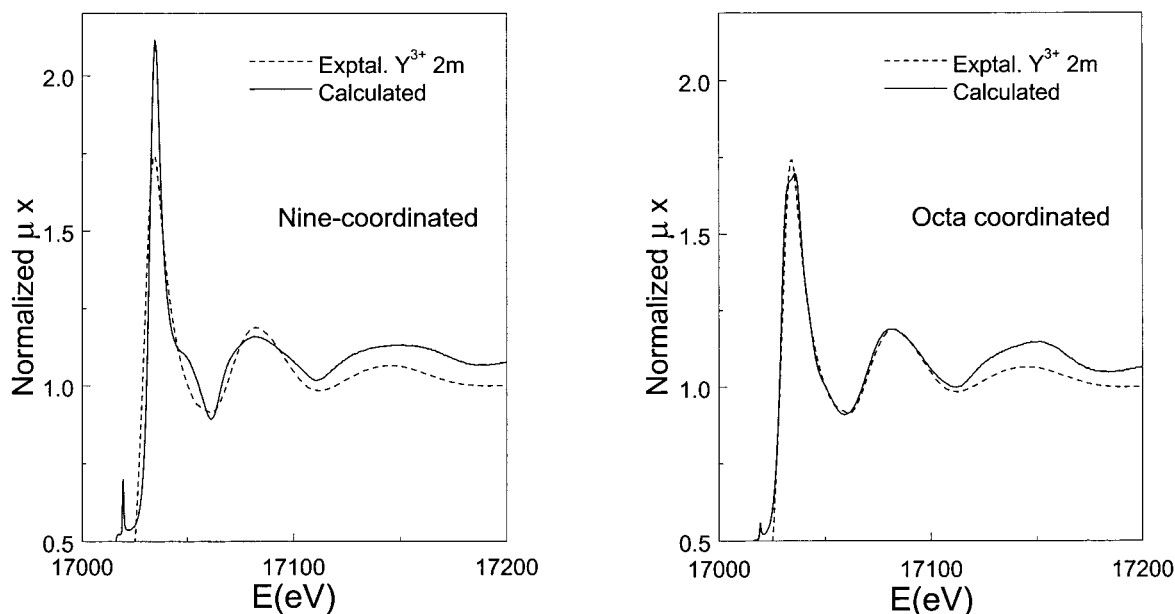


Figure 7. Experimental XANES spectra of 2 m YBr_3 aqueous solution in liquid state (dashed line) and computed spectra (solid line) using the self-consistent field approach and Dirac–Hara exchange and correlation potential with the imaginary part of Hedin–Lundqvist one, for the nine-coordinated and eight-coordinated aquacomplexes.

the photoabsorbing yttrium (radius $\sim 5 \text{ \AA}$) and using several final-state potentials. In the first approach the potential was built on the basis of $Z+1$ and X_α approximations; the theoretical spectrum thus obtained reproduces all of the features present in the experimental spectrum, in particular, the shoulder on the high-energy side of the absorption white line. However, despite of the good agreement obtained in reproducing all of the features present in the experimental spectra, this calculation fails to reproduce the energy separation between the various resonances. Indeed, it seems that the energy scale of the theoretical spectrum is “contracted” with respect to that of the experimental spectrum. This result, showing the calculated absorption maxima falling short of the observed maxima, has been already pointed out in previous investigations and is associated with the energy independence of the X_α exchange potential. Therefore, one of the possibilities to improve the theoretical simulation may be the use of different exchange-correlation contributions to the final-state potential. Subsequently, the same calculation was performed by using the Hedin–Lundqvist complex potential, which led to a better reproduction of the intensity of the absorption features beyond the white line, as the use of a complex potential introduces the damping of the multiple-scattering contributions to the spectrum. However, the relative intensity of the two contributions to the absorption main peak is not satisfactory and the contraction of the energy scale still persists.

Trying to solve these problems, the performance of the Dirac–Hara potential was tested, leading to the correct reproduction of both the experimental resonances and their energy separation. However, the white line intensity is not satisfactory at all. To overcome this discrepancy new calculations using a self-consistent field final-state potential incorporating the Dirac–Hara exchange and correlation potential were performed. The computed XANES profile is essentially the same, as regards the number and energy position of the features, but now there is a strong improvement on the width and height of the white line, in fact, it gives rise to a narrower and higher white line resembling the experimental data. Finally, the imaginary part of the Hedin–Lundqvist potential was added to the Dirac–Hara potential, to take into account the inelastic losses of the

photoelectron. As shown in Figure 6, the experimental spectrum is well modeled by this last computation.

The findings of these calculations can be summarized as follows: (i) the use of the self-consistent field potential in the ab initio calculations is crucial to account for the shape and intensity of the white line exhibited by the Y K-edge experimental spectrum of solid yttrium triflate; (ii) the Dirac–Hara exchange and correlation potential leads to an accurate reproduction of the experimental energy scale; and (iii) incorporating the imaginary part of the Hedin–Lundqvist exchange and correlation potential to the previous one leads to a satisfactory simulation of the photoelectron damping, providing a good agreement between the computational and experimental data for solid yttrium(III) triflate. Following these findings we now address the determination of the local structure of yttrium(III) cations in aqueous solution.

The same procedure described for the solid compound was followed to carry out the computations of two clusters corresponding to the different arrangements proposed for the solution: a regular tricapped trigonal prism, corresponding to the 9-fold structure, and a square antiprism as model for the 8-fold coordination. In both cases, the distance Y–O has been set equal to 2.35 \AA , the value obtained by EXAFS.

The final results of the computation process are shown in Figure 7a for the case of nine-coordinated cluster and in Figure 7b for the eight-coordinated yttrium complex. This figure clearly shows that the experimental spectrum for the solution is better reproduced by the XANES spectrum computed for the eight-coordinated model. Indeed, in the case of the nine-coordinated cluster the computation reveals a strong peak on the high-energy side of the main absorption peak, similar to that observed in the triflate. Also, for the nine-coordinated cluster the energy separation between the white line and the first resonance is too short as compared with the experimental data.

The results of the computations are then consistent with the hypothesis of yttrium(III) being eight-coordinated in aqueous solution. Additionally, we might conclude that while EXAFS cannot yield conclusive information regarding the coordination number of yttrium hydrates, XANES is capable of solving this problem due to its sensitivity to the site-symmetry of the

absorbing atom. Thus, while a variation between 8 and 9 for coordination number in EXAFS affects only the amplitude of the signal, when calculating the XANES region the different atomic arrangements modify the shape of the whole absorption spectrum.

Concluding Remarks

From the foregoing results, the hydration structure of yttrium(III) in solution can be extracted. Eight water molecules are located around the central cation at 2.35 Å, forming a symmetric square antiprism. This structure is the same in a wide range of concentrations, from highly dilute, 0.005 m, up to concentrated, 2.0 m, aqueous solutions. The polyhedron structure is found to be constant in a 2.0 m solution measured at liquid nitrogen temperature. We have found no evidence for ion-pair formation, even in the case that there is just enough water in the solution to hydrate each ion.

This study has shown the capabilities and limitations of the EXAFS technique and in which manner these limitations can be overcome using the information contained in the XANES region and appropriate quantum mechanical models.

Acknowledgment. We thank I. Watanabe, H. Sakane, T. Miyanaga, and J. M. Martínez for their assistance during the recording of the EXAFS spectra. M. Nomura is acknowledged for his help with the measurements of the glassy solutions, and D. Bowron for helpful discussions. Thanks are also due to the Photon Factory of the Institute of Material Structure Science Project (project number 95-G215) at KEK, Tsukuba for beam-time allocation, and to the Spanish DGICYT (project number PB95-549) for financial support.

References and Notes

- Richens, D. T. *The Chemistry of Aqua Ions*; Wiley: Chichester, 1997.
- Marcus, Y. *Ion Solvation*; Wiley: Chichester, 1986.
- Ohtaki, H.; Yamatera, H. *Structure and Dynamics of Solutions*; Elsevier: Amsterdam, 1992.
- Shannon, R. D. *Acta Crystallogr.* **1976**, A32, 751.
- Habenschuss, A.; Spedding, F. H. *J. Chem. Phys.* **1979**, 70, 442.
- Harrowfield, J. M.; Kepert, D. L.; Patrick, J. M.; White, A. H. *Aust. J. Chem.* **1983**, 36, 483.
- Cotton, F. A.; Davison, A.; Day, V. W.; Fredrich, M. F.; Orvig, C.; Swanson, R. *Inorg. Chem.* **1982**, 21, 1211.
- Bukowska-Strzyzewska, M.; Tosic, A. *Acta Crystallogr.* **1982**, B38, 950.
- Templeton, D. H.; Carter, G. F. *J. Phys. Chem.* **1954**, 58, 940.
- Díaz-Moreno, S.; Matínez, J. M.; Muñoz-Páez, A.; Sakane, H.; Watanabe, I. *J. Phys. Chem.* **1998**, 102, 7435.
- Johansson, G.; Wakita, H. *Inorg. Chem.* **1985**, 24, 3047.
- Matsubara, E.; Okuda, K.; Waseda, Y. *J. Phys.: Condens. Matter* **1990**, 2, 9133.
- De Barros Marques, M. I.; Alves Marques, M.; Resina Rodrigues, J. *J. Phys.: Condens. Matter* **1992**, 4, 7679.
- (a) Díaz-Moreno, S. *Estudio de la estructura de complejos metálicos en disolución mediante Espectroscopías de Absorción de Rayos X*. Ph.D. Thesis, University of Sevilla (Spain), 1998; Chapter IV.5. (b) Díaz-Moreno, S.; Muñoz-Páez, A.; Chaboy Nalda, J. *Proc. 4th Liquid Matter Conference*, Europhysics Conference Abstract, Volume 23C, Granada (Spain), 1999, pp 6–26.
- Mayer, I.; Zolotov, S. *J. Inorg. Nucl. Chem.* **1965**, 27, 1905.
- Nomura, M.; Yamaguchi, T. *J. Phys. Chem.* **1988**, 92, 6157.
- Yamaguchi, T.; Nomura, M.; Wakita, H.; Ohtaki, H. *J. Chem. Phys.* **1988**, 89, 5153.
- Sánchez Marcos, E.; Gil, M.; Sánchez Marcos, A.; Martínez, J. M.; Muñoz-Páez, A. *Rev. Sci. Ins.* **1994**, 65, 2153.
- Cook, J. W.; Sayers, D. E. *J. Appl. Phys.* **1981**, 52, 5024.
- Vaarkamp, M.; Linders, J. C.; Koningsberger, D. C. *Phys. B* **1995**, 208, 209, 159.
- Lyttle, F. W.; Sayers, D. E. *Physica B* **1988**, 158, 701.
- Zabinsky, S. I.; Rehr, J. J.; Ankudinov, A.; Albers, R. C.; Eller, M. J. *Phys. Rev. B* **1995**, 52, 2995.
- Natoli, C. R.; Benfatto, M., unpublished.
- Natoli, C. R.; Benfatto, M. *J. Phys. (Paris) Colloq.* **1986**, 47, C8–11.
- Tyson, T. A.; Hodgson, K. O.; Natoli, C. R.; Benfatto, M. *Phys. Rev. B* **1994**, 46, 5997.
- Mattheis, L. F. *Phys. Rev. A* **1964**, 133, 1399. Mattheis, L. F. *Phys. Rev. A* **1964**, 134, 970.
- Clementi, E.; Roetti, C. *Atomic Data and Nuclear Data Tables* **1974**, 14, 177.
- Slater, J. C. *The Self-consistent Field for Molecules and Solids; Quantum Theory of Molecules and Solids*; McGraw-Hill: New York, 1979.
- Hedin, L.; Lundqvist, B. I. *J. Phys.* **1971**, C4, 2064.
- (a) Hara, S. *J. Phys. Soc. Jpn.* **1967**, 22, 710. (b) Gunnella, R.; Benfatto, M.; Marcelli, A.; Natoli, C. R. *Solid State Commun.* **1990**, 76, 109.
- Muñoz-Páez, A.; Sanchez-Marcos, E. *J. Am. Chem. Soc.* **1992**, 89, 5153.
- Lincoln, S. F. *Adv. Inorg. Bioinorg. Mech.* **1986**, 4, 217.
- Cossy, C.; Merbach, A. E. *Pure Appl. Chem.* **1988**, 60, 1785.
- Cossy, C.; Barnes, A. C.; Enderby, J. E.; Merbach, A. E. *J. Chem. Phys.* **1989**, 90, 3254.
- Yamaguchi, T.; Niihara, M.; Takamaku, T.; Wakita, H.; Kanno, H. *Chem. Phys. Lett.* **1997**, 247, 485.
- Chaboy, J.; Tysson, T. A. *Phys. Rev. B* **1994**, 49, 5869.
- Chaboy, J.; Marcelli, A.; Tysson, T. A. *Phys. Rev. B* **1994**, 49, 11652.
- Díaz-Moreno, S.; Muñoz-Páez, A.; Martínez, J. M.; Pappalardo, R. R.; Sánchez Marcos, E. *J. Am. Chem. Soc.* **1996**, 118, 12654.
- Brady, G. W. *J. Chem. Phys.* **1960**, 33, 1079.
- Ishiguro, S.; Kato, K.; Takahashi, R.; Nakasone, S. *Rare Earths* **1995**, 27, 61.
- Ishiguro, S.; Umabayashi, Y.; Kato, K.; Nakasone, S.; Takahashi, R. *Phys. Chem. Chem. Phys.* **1999**, 1, 2725.
- Takahashi, R.; Ishiguro, S. *J. Chem. Soc., Faraday Trans.* **1991**, 87, 3379.
- Solera, J. A.; Garcia, J.; Proietti, G. *Phys. Rev. B* **1995**, 51, 2678.
- Chaboy, J.; Garcia, J.; Marcelli, A.; Ruiz-Lopez, M. F. *Chem. Phys. Lett.* **1990**, 174, 389.
- D'Angelo, P.; Di Nola, A.; Giglio, E.; Mangani, M.; Pavel, N. V. *J. Phys. Chem.* **1995**, 99, 5471.